ISSN 0962-1083

VOLUME 22
NUMBER 12
JUNE
2013

MOLECULAR ECOLOGY

Published by
Wiley Blackwell

MOLECULAR ECOLOGY

VOLUME 22, NUMBER 12, JUNE 2013

NEWS AND VIEWS

Perspectives

3191 Intertidal population genetic dynamics at a microgeographic seascape scale
Z.-M. Hu

3195 Hybridization and the porous genome: patterns of isolation and introgression in manakins
S. Yeaman

Opinion

3198 Community genetics in the time of next-generation molecular technologies
F. Gugerli, R. Brandl, B. Castagneyrol, A. Franc, H. Jactel, H.-P. Koelewijn, F. Martin, M. Peter, K. Pritsch, H. Schröder, M. J. M. Smulders, A. Kremer, B. Ziegenhagen & Evoltree Jera3 Contributors

Comment

3208 Conserving genetic diversity in the honeybee: Comments on Harpur *et al.* (2012)
P. De la Rúa, R. Jaffé, I. Muñoz, J. Serrano, R. F. A. Moritz & F. B. Kraus

Reply

3211 Admixture increases diversity in managed honey bees: Reply to De la Rúa *et al.* (2013)
B. A. Harpur, S. Minaei, C. F. Kent & A. Zayed

INVITED REVIEWS AND META-ANALYSES

3216 Annotated genes and nonannotated genomes: cross-species use of Gene Ontology in ecology and evolution research
C. R. Primmer, S. Papakostas, E. H. Leder, M. J. Davis & M. A. Ragan

ORIGINAL ARTICLES

Population and Conservation Genetics

3242 Intergametophytic selfing and microgeographic genetic structure shape populations of the intertidal red seaweed *Chondrus crispus*
S. A. Krueger-Hadfield, D. Roze, S. Mauger & M. Valero

3261 Tracking climate change in a dispersal-limited species: reduced spatial and genetic connectivity in a montane salamander
G. Velo-Antón, J. L. Parra, G. Parra-Olea & K. R. Zamudio

3279 The demographic history of populations experiencing asymmetric gene flow: combining simulated and empirical data
I. Paz-Vinas, E. Quéméré, L. Chikhi, G. Loot & S. Blanchet

Molecular Adaptation

3292 Evolutionary history and genetic parallelism affect correlated responses to evolution
M. Le Gac, T. F. Cooper, S. Cruveiller, C. Médigue & D. Schneider

Speciation and Hybridization

3304 The genomic consequences of adaptive divergence and reproductive isolation between species of manakins
T. L. Parchman, Z. Gompert, M. J. Braun, R. T. Brumfield, D. B. McDonald, J. A. C. Uy, G. Zhang, E. D. Jarvis, B. A. Schlinger & C. A. Buerkle

Phylogeography

3318 Divergent evolutionary histories of two sympatric spruce bark beetle species
C. Bertheau, H. Schuler, W. Arthofer, D. N. Avtzis, F. Mayer, S. Krumböck, Y. Moodley & C. Stauffer

3333 Gene trees, species trees and Earth history combine to shed light on the evolution of migration in a model avian system
G. Voelker, R. C. K. Bowie & J. Klicka

3345 Ecological coassociations influence species' responses to past climatic change: an example from a Sonoran Desert bark beetle
R. C. Garrick, J. D. Nason, J. F. Fernández-Manjarrés & R. J. Dyer

3362 Stepping-stone expansion and habitat loss explain a peculiar genetic structure and distribution of a forest insect
A. Cassel-Lundhagen, C. Ronnås, A. Battisti, J. Wallén & S. Larsson

3376 Phylogeography of Silver Pheasant (*Lophura nycthemera* L.) across China: aggregate effects of refugia, introgression and riverine barriers
L. Dong, G. Heckel, W. Liang & Y. Zhang

Kinship, Parentage and Behaviour

3391 Extreme genetic mixing within colonies of the wood-dwelling termite *Kalotermes flavicollis* (Isoptera, Kalotermitidae)
A. Luchetti, F. Dedeine, A. Veloná and B. Mantovani

Ecological Interactions

3403 Host plant genus-level diversity is the best predictor of ectomycorrhizal fungal diversity in a Chinese subtropical forest
C. Gao, N.-N. Shi, Y.-X. Liu, K. G. Peay, Y. Zheng, Q. Ding, X.-C. Mi, K.-P. Ma, T. Wubet, F. Buscot & L.-D. Guo

3415 Soil bacterial community succession during long-term ecosystem development
K. Jangid, W. B. Whitman, L. M. Condron, B. L. Turner & M. A. Williams

3425 **Erratum**

Information on this journal can be accessed at http://wileyonlinelibrary.com/journal/mec

The journal is covered by *AGRICOLA, Chemical Abstracts, Current Awareness Biological Sciences* and *Current Contents.*

This journal is available at *Wiley Online Library.* Visit http://wileyonlinelibrary.com to search the articles and register for table of contents e-mail alerts.

WILEY Blackwell

MOLECULAR ECOLOGY

Molecular Ecology (2013) **22**, 3376–3390 doi: 10.1111/mec.12315

Phylogeography of Silver Pheasant (*Lophura nycthemera* L.) across China: aggregate effects of refugia, introgression and riverine barriers

LU DONG*, GERALD HECKEL†‡, WEI LIANG§ and YANYUN ZHANG*

**Ministry of Education Key Laboratory for Biodiversity and Ecological Engineering, College of Life Sciences, Beijing Normal University, Beijing 100875, China, †Computational and Molecular Population Genetics, Institute of Ecology and Evolution, University of Bern, Baltzerstrasse 6, 3012 Bern, Switzerland, ‡Swiss Institute of Bioinformatics, Genopode, 1015 Lausanne, Switzerland, §Ministry of Education Key Laboratory for Tropical Animal and Plant Ecology, College of Life Sciences, Hainan Normal University, Haikou 571158, China*

Abstract

The role of Pleistocene glacial cycles in forming the contemporary genetic structure of organisms has been well studied in China with a particular focus on the Tibetan Plateau. However, China has a complex topography and diversity of local climates, and how glacial cycles may have shaped the subtropical and tropical biota of the region remains mostly unaddressed. To investigate the factors that affected the phylogeography and population history of a widely distributed and nondeciduous forest species, we analysed morphological characters, mitochondrial DNA sequences and nuclear microsatellite loci in the Silver Pheasant (*Lophura nycthemera*). In a pattern generally consistent with phenotypic clusters, but not nominal subspecies, deeply divergent mitochondrial lineages restricted to different geographic regions were detected. Coalescent simulations indicated that the time of main divergence events corresponded to major glacial periods in the Pleistocene and gene flow was only partially lowered by drainage barriers between some populations. Intraspecific cytonuclear discordance was revealed in mitochondrial lineages from Hainan Island and the Sichuan Basin with evidence of nuclear gene flow from neighbouring populations into the latter. Unexpectedly, hybridization was revealed in Yingjiang between the Silver Pheasant and Kalij Pheasant (*Lophura leucomelanos*) with wide genetic introgression at both the mtDNA and nuclear levels. Our results highlight a novel phylogeographic pattern in a subtropical area generated from the combined effects of climate oscillation, partial drainage barriers and interspecific hybridization. Cytonuclear discordance combined with morphological differentiation implies that complex historical factors shaped the divergence process in this biodiversity hot spot area of southern China.

Keywords: genetic introgression, Hainan island, hydrographic barrier, phylogeographic pattern, Pleistocene refugia, Silver Pheasant

Received 23 November 2011; revision received 12 March 2013; accepted 14 March 2013

Introduction

Past geologic events and climatic fluctuations in the Pleistocene had profound impacts on the phylogeographic structure and genetic patterns of organisms (Hewitt 2000, 2004; van Tuinen & Dyke 2004; Song *et al.* 2009). This has resulted in high diversity in subtropical and tropical regions of southern China, a major biodiversity hotspot (Crowe *et al.* 2006). Although this region has never been covered by ice sheets, it experienced cooler and drier climates during the Pleistocene (Howard 1997), and it was also affected by the uplift of the Qinghai–Tibet plateau (Cheng *et al.* 2001). The tremendous climatic changes during this period influenced the distribution and evolution of many plants and animals (Dyke & van

Correspondence: Yanyun Zhang, Fax: +86 10 588 053 99; E-mail: zhangyy@bnu.edu.cn

Tuinen 2004; Huang *et al.* 2010; Ding *et al.* 2011). Previous studies regarding genetic differentiation and historical demography of the avifauna of this region indicate typically multiple refugia during glacial periods (Fuchs *et al.* 2007; Li *et al.* 2009; Song *et al.* 2009; Dai *et al.* 2011). However, with the exception of studies on a few amphibians (Zhang *et al.* 2010a,b) and an endemic insular species (Li *et al.* 2010), there has been little research on whether geographic factors have prevented gene flow and maintained postdivergence isolation of species in this region.

Although evidence of long-term isolation by drainage systems such as rivers and straits is mixed, several studies have indicated that such geographic features can act as barriers to gene flow in birds and mammals (Aleixo 2004; Hayes & Sewlal 2004; Anthony *et al.* 2007; Nicolas *et al.* 2011). Understanding the extent to which riverine barrier effects may be heightened for populations in multiple refugia would help explain the maintenance and generation of diversity under conditions of Pleistocene climate oscillation. Moreover, there has been a tremendous increase in hybridization and introgression-related avian research in Europe and North America (e.g. Vallender *et al.* 2007; Qvarnström *et al.* 2010; Brelsford *et al.* 2011; Hermansen *et al.* 2011; Rheindt & Edwards 2011), but knowledge on how this process has impacted natural allopatric avian species and lineages in East Asia is limited. Insight into this issue is important to evaluate the comprehensive mechanisms of diversification processes (Hennache *et al.* 2003; Rheindt & Edwards 2011), and phylogeographic analyses on a widely distributed species in this highly diverse area have the potential to advance our knowledge substantially.

The Silver Pheasant (*Lophura nycthemera* L.) is widely distributed in southern China and the Indo-Chinese peninsula and includes 15 subspecies, nine of which occur in China (Johnsgard 1999). Delacour (1948) used the plumage pattern of the upper part of the male (mainly the numbers of white and black stripes) and the presence of topographic barriers to establish these taxa and their relationships. Briefly, the southern subspecies *L. n. annamensis*, *L. n. lewisi*, *L. n. engelbachi* and *L. n. beli* have larger numbers of wide black stripes compared to northern subspecies except *L. n. rufipes*, which is distributed in south-western Yunnan (Dong & Zhang 2011). However, McGowan & Panchen (1994) proposed that this species was probably oversplit because seven subspecies (*L. n. rufipes*, *L. n. occidentalis*, *L. n. ripponi*, *L. n. jonesi*, *L. n. beaulieui*, *L. n. nycthemera* and *L. n. fokiensis*) had clinal plumage patterns that did not merit separation into a series of distinct forms. They also suggested that the most ancestral plumage pattern occurs in the aggregate range of *L. nycthemera* and the Kalij Pheasant *Lophura leucomelanos* around the Irrawaddy River and inferred that the Silver Pheasant originated in the west and then dispersed eastward. This is generally consistent with the inference that Silver Pheasant split with Kalij Pheasant about 1.4 Mya based on the reconstruction of the *Lophura* phylogeny (Randi *et al.* 2001). A previous study revealed two clades in mitochondrial DNA (mtDNA) sequences from the control region (CR) and partial cytochrome b (cyt *b*) by investigating five subspecies of Silver Pheasant (Moulin *et al.* 2003). However, the sampling scheme (only 24 individuals, including 20 from captive breeders) provided very limited possibilities to reveal phylogeographic patterns and test for historical climatic and topological impact on population divergence in Silver Pheasant.

To investigate the impact of late Pleistocene refugia and riverine barrier dynamics on population genetic differentiation, we analysed phylogeographic patterns and processes in nine Silver Pheasant subspecies in China. We focused on samples from Hainan Island and populations separated by different rivers like the Yangtze or the Red River on the continent, which allowed us to test hypotheses regarding genetic breaks associated with potential barriers. Specifically, we identified major geographically defined evolutionary lineages in Silver Pheasant based on a combination of morphology and genetic data and performed coalescence simulations to test whether intraspecific divergence was related to Pleistocene climate oscillations or barrier effects of major rivers.

Materials and methods

Field work and genetic sampling

Between 2007 and 2010, we collected 170 blood and fresh feather samples of *L. nycthemera* at 21 localities throughout the pheasant's range in China from 97.6°E to 119.6°E and 19.1°N to 30.1°N, covering all nine subspecies in the region, and 10 *L. leucomelanos lathami* tissue samples from the border of China and Myanmar (for details, see Fig. 1; Table 1). Blood samples were collected by loop-trapping with permission from local wildlife management authorities and stored in 95% ethanol in the field. Feather samples were collected during the moulting season and kept in envelopes that were stored in a dry place. All samples were transferred to a freezer at −80 °C for long-term storage.

DNA was extracted using a TIANamp Genomic DNA Kit (Tiangen Biotech, China) and resuspended in TE buffer. For feathers in good condition, the blood clot in the superior umbilicus was used to extract DNA; for those in poor condition, the whole calamus was used (Ksepka 2009).

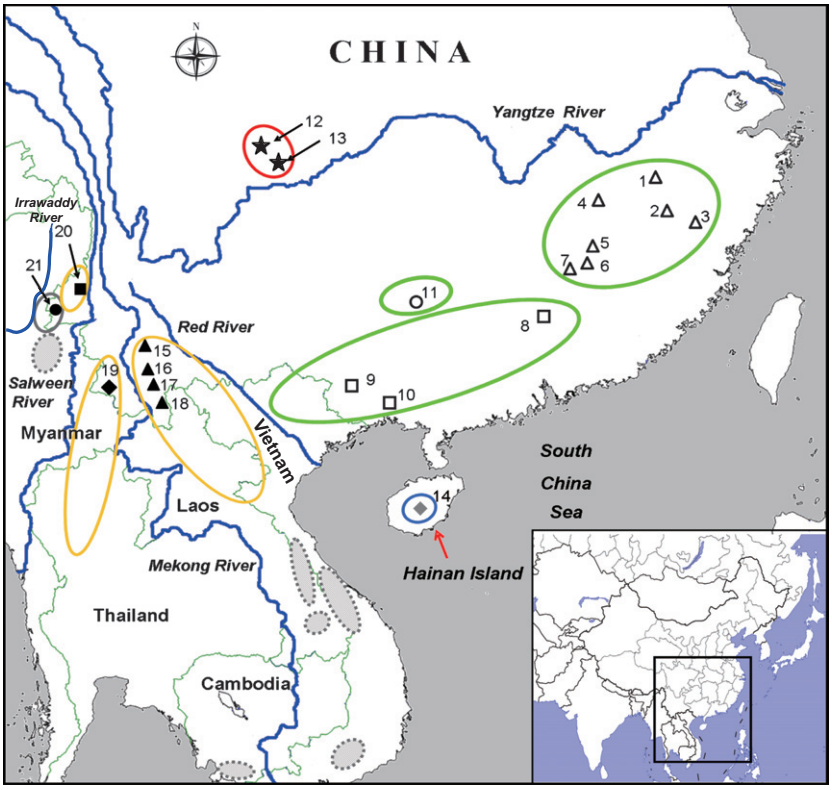

Fig. 1 Sampling localities of Silver Pheasant (*Lophura nycthemera*) across its range in China. The study area is shown on a map of China (inset: lower right). Numbers correspond to map references and the sampling localities in Table 1. Different symbols represent subspecies and ellipses show the rough distribution of subspecies. △: *L. n. fokiensis*; □: *L. n. nycthemera*; ○: *L. n. rongjiangensis*; ★: *L. n. omeiensis*; ♦: *L. n. whiteheadi*; ▲: *L. n. beaulieui*; ♦: *L. n. jonesi*; ■: *L. n. occidentalis*; ●: *L. n. rufipes*. Colours of ellipses correspond to five mitochondrial DNA clades (see Fig. 2), and filling of symbols (white, grey and black) indicates the three nuclear clades (see Figs 3 and 4). Grey ellipses indicate unsampled subspecies. The main rivers in the distribution area are also shown on the map.

mtDNA sequencing

Almost the entire *cyt b* gene (1080 bp) and CR (1071 bp) were sequenced. Polymerase chain reaction (PCR) amplifications were carried out using Phasianidae-specific primers: PHDH and PHDL for CR (Randi & Lucchini 1998), and MH15907 and ML15131 for cyt *b* (Shen *et al.* 2010). PCR was performed in a final volume of 25 μL and contained 1.25 U Taq DNA polymerase (Takara, Kyoto, Japan), 1 × PCR buffer (Takara, Japan), 0.4 mM dNTP (Takara), 0.4 μL of both primers (10 pM), 50–100 ng DNA template and ddH_2O. PCR conditions were as follows: denaturation at 94 °C for 5 min, followed by 35 cycles of amplification consisting of 94 °C for 30 s, 53 °C for 1 min and 72 °C for 90 s, with a final elongation for 10 min at 72 °C.

Polymerase chain reaction products were purified with a Wizard™ PCR Preps DNA purification kit (Promega, Madison, WI, USA) and subsequently sequenced with each of the primers. The sequencing programme consisted of 30 cycles of denaturation at 96 °C for 20 s, annealing at 50 °C for 10 s, extension at 60 °C for 90 s and fragment separation on an ABI 3730 automated sequencer (Applied Biosystems, Foster City, CA, USA). The chromatogram of each sequence was proofread by eye with the aid of the program SEQUENCHER version 4.0 (Gene Codes Co., Ann Arbor, MI, USA). Ten randomly selected samples were resequenced for two mtDNA fragments to check the consistency and accuracy of the PCR and sequencing processes.

Microsatellite genotyping

Eleven microsatellite loci, including six cross-species amplifying loci and five novel loci, were genotyped. M1, M2 and M5 isolated from *Gallus gallus* were available in *Lophura* species (Hennache *et al.* 2003). T05, T32 and T40 isolated from *Tragopan temminckii* (Zhou & Zhang 2009), with P3, P5, P9, P17 and P18 isolated from *L. nycthemera* (Dong *et al.* unpublished data), were developed using the same protocol in the same laboratory (College of Life Sciences, Beijing Normal University, Beijing, China). These loci were assigned to two multiplex sets (set 1: M1, M2, P3, P17 and P18; set 2: P5, M5, T05 and T32) and two separately amplified loci (P9 and T40). The multiplex sets were amplified using a multiplex kit (Qiagen, Valencia, CA, USA), with the following PCR protocol: an initial denaturing step of 95 °C for 15 min, followed by 30 cycles of 30 s at 94 °C, 90 s at 57 °C and 60 s at 72 °C, with a final extension step of 30 min at 60 °C. The single locus T40 was amplified according to Zhou & Zhang (2009). GeneScanTM-500LIZ™ (Applied Biosystems) was added to the diluted PCR product to determine the allele size. Fragment sizes were obtained on an Applied Biosystems 3730 and scored using GENEMAPPER version 3.7 (Applied Biosystems). Fifty samples (28%) were amplified twice to check the accuracy, and all samples were scored twice independently to ensure consistency of genotyping (Hahne *et al.* 2011).

Table 1 Genetic diversity in Silver Pheasants estimated from 2051 bp mtDNA sequence (control region and cyt *b*) and 11 microsatellite loci. Samples analysed are listed as subspecies, population labels (details in Table S1, Supporting information) and number of individuals analysed for mtDNA (N_{mt}) and microsatellite loci (N_{nuc}). For mtDNA, the number of haplotypes (N_H), haplotype diversity (H) and nucleotide diversity ($\pi \pm$ SD, in per cent) were calculated. For microsatellites, the means of expected heterozygosity (H_E), observed heterozygosity (H_O) and allelic richness (A_R) are indicated at the population level

			Mitochondrial DNA				Microsatellites			
Subspecies	Map ref.	Pop. labels	N_{mt}	N_H	H	$\pi \pm$ SD (%)	N_{nuc}	H_E	H_O	A_R
L. n. fokiensis	1	AH	4	2	0.500	0.07 ± 0.037	3	0.630	0.576	3.09
	2	WYS	9	7	0.944	0.171 ± 0.023	11	0.576	0.446	5.09
	3	ZJ	3	2	0.667	0.062 ± 0.029	7	0.606	0.528	3.73
	4	GS	15	4	0.752	0.168 ± 0.016	23	0.561	0.407	5.18
	5	JG	1	1	n.a.	n.a.	2	n.a.	n.a.	n.a.
	6	SCH	2	2	1	0.28 ± 0.14	2	n.a.	n.a.	n.a.
	7	HU	8	6	0.929	0.171 ± 0.03	9	0.605	0.455	4.73
L. n. nycthemera	8	SG	2	2	1	0.14 ± 0.07	0	n.a.	n.a.	n.a.
	9	GX	0	n.a.	n.a.	n.a.	1	n.a.	n.a.	n.a.
	10	GX	1	1	n.a.	n.a.	1	n.a.	n.a.	n.a.
L. n. rongjiangensis	11	GZ	3	3	1.000	0.124 ± 0.046	3	0.521	0.485	2.82
L. n. omeiensis	12	HY	4	2	0.667	0.311 ± 0.095	4	0.635	0.659	3.09
	13	LJS	9	5	0.861	0.279 ± 0.028	9	0.624	0.577	4.35
L. n. whiteheadi	14	HN	14	8	0.923	0.122 ± 0.013	26	0.495	0.406	4.45
L. n. beaulieui	15	AL	1	1	n.a.	n.a.	1	n.a.	n.a.	n.a.
	16	NE	7	4	0.810	0.262 ± 0.042	7	0.634	0.571	4.18
	17	PW	4	4	1.000	0.187 ± 0.045	4	0.731	0.659	4.09
	18	BN	7	6	0.952	0.262 ± 0.045	6	0.703	0.584	5.09
L. n. jonesi	19	CY	8	8	1.000	0.366 ± 0.05	9	0.723	0.579	5.82
L. n. occidentalis	20	GLG	1	1	n.a.	n.a.	1	n.a.	n.a.	n.a.
L. n. rufipes	21	YJ	30	18	0.917	1.669 ± 0.112	39	0.693	0.544	9.18
L. leucomelanos	21	Kalij	10	8	0.956	0.401 ± 0.041	10	0.633	0.541	4.64
Total			143	86	0.986	1.499 ± 0.078	178	0.736	0.501	14.73

Genetic polymorphism

Mitochondrial DNA sequences were aligned with Clustal W in MEGA 5.0 (Tamura *et al*., 2011) and refined manually. DNASP 5.0 (Kimball & Braun 2008) was used to calculate the number of segregating sites and haplotypes, haplotype (H) and nucleotide diversity (π). The homogeneity test in PAUP* 4.0b10 (Swofford 2001) was conducted on concatenated CR and cyt *b* haplotype sequences. No significant heterogeneity was detected between the two partitions ($P = 0.29$, 1000 replicates), and thus, they were analysed as a combined data set.

Number of microsatellite alleles, allele frequencies and observed and expected heterozygosities were calculated for each locus and each population using ARLEQUIN 3.0 (Excoffier *et al.* 2005). ARLEQUIN was also used to test for statistically significant deviations from Hardy–Weinberg and genotypic linkage equilibrium. A sequential Bonferroni method (Bowen *et al.* 2002) was utilized to correct for multiple testing. Global F_{ST} and pairwise F_{ST} were calculated at the population level. Then, to improve statistical power, we pooled populations from close localities that did not show pairwise structure (pairwise $F_{ST} < 0.01$) into demes, as follows: HY and LJS were combined as a Sichuan population (SC), and PW and NE were combined as a PE population. Analyses of molecular variance (AMOVA) were performed with the same groupings as in the mtDNA analyses using ARLEQUIN.

Phylogeographic and population structure

Three CR and cyt *b* sequences from *L. leucomelanos* (AJ300153, AF314642), *L. swinhoii* (AJ300155, AF314644) and *L. hatinhensis* (AJ300150, AF314640) were used as out-groups because of their close phylogenetic relationship with *L. nycthemera* (Randi *et al.* 2001). For the concatenated mtDNA sequences, models of nucleotide substitution were tested using JMODELTEST v.0.1.1 (Guindon & Gascuel 2003; Posada 2008), and a corrected Akaike information criterion (AICc) was employed to determine the best-fit model. Bayesian trees were constructed with MRBAYES v.3.1.2 (Huelsenbeck & Ronquist 2001; Ronquist & Huelsenbeck 2003) to generate Bayesian posterior probabilities (BPP) for phylogenetic inferences. When specific models selected by jModeltest were not implemented in MRBAYES, the closest general model in

MrBayes was used (Kindler *et al.* 2012). Two independent Markov chain Monte Carlo (MCMC) runs, each with six chains for 5 million generations and sampled every 1000 steps, were performed. Convergence onto the stationary distribution was confirmed by checking whether the deviation of split frequencies was below 0.01 between the two independent runs. The first 1250 trees were discarded as burn-in based on the stationarity of ln L as assessed using TRACER v.1.4.1 (Rambaut & Drummond 2007). In addition, we used the program PHYML v.3.0 (Guindon & Gascuel 2003) to reconstruct maximum-likelihood relationships among the haplotypes and employed the approximate likelihood ratio test (aLRT) (Anisimova & Gascuel 2006) to estimate node support. Furthermore, maximum parsimony analyses were conducted using MEGA 5.0 to examine whether different phylogenetic criteria would alter the topology. In addition, a maximum parsimony median-joining network was used to illustrate genealogical relationships among haplotypes with Network 4.5.1 (Bandelt *et al.* 1999).

To further assess genetic structure among individuals, we conducted principle coordinate analysis (PCoA) on a genetic distance matrix generated from the microsatellite binary data matrix implemented in GENALEX 6.1 (Peakall & Smouse 2006). Moreover, we examined the patterns of population structure using the individual assignment test in the program STRUCTURE 2.3.1 (Pritchard *et al.* 2000). This program uses Bayesian inference to generate posterior probabilities of assignment for each individual to a number of genetic clusters (K), which are characterized by a set of allele frequencies at each locus. Considering our intraspecies-level analysis and the potential for gene flow between populations, an admixture model was selected for the assignment. We performed 10 independent runs with 1 million MCMC iterations for $K = 1$–9 each and discarded the first 100 000 iterations as burn-in. The optimal value of K was calculated according to the method of Evanno *et al.* (2005).

ARLEQUIN 3.5 was used to calculate global and pairwise Φ_{ST} estimates using the Tamura–Nei substitution model. Levels of differentiation among populations were assessed using pairwise F_{ST} and AMOVA with ARLEQUIN. The Tamura & Nei (1993) model was used because it has the closest relation to the HKY model. Two scenarios for AMOVA were defined based on the haplogroups revealed by mtDNA phylogenetic analyses and island-continent isolation of populations.

Neutrality test and mismatch analysis

Tajima's D and Fu's F tests implemented in ARLEQUIN were used to detect departures from the mutation-drift equilibrium indicative of changes in historical demography and natural selection. Mismatch analyses were conducted in ARLEQUIN to characterize the magnitude and timing of past changes in population size. Each mismatch distribution was compared to the expected distribution under a model of sudden population expansion. For a population undergoing exponential growth, the mismatch distribution is expected to have a bell-shaped curve. The validity of the estimated demographic model was tested by determining the distribution of the sum of squared differences (SSD) between the observed and the estimated mismatch distribution. The significance of SSD was assessed with 10 000 parametric bootstraps. The time to the expansion of each clade was derived from the estimation of τ, according to the equation $\tau = 2\mu kt$, where τ is the mode of the mismatch distribution, μ is the nucleotide mutation rate (1.19% per Myr as below) and k is the number of nucleotides.

Time to the most recent common ancestor and divergence time

BEAST 1.6.1 (Drummond & Rambaut 2007) was used to estimate the time to the most recent common ancestor (TMRCA) of clades in *L. nycthemera*. The HKY+I+G model with a prior of a constant size was selected. To account for rate variation among lineages, the uncorrelated lognormal model was selected. Independent MCMC analyses were run for 10^8 steps, sampling every 10^3 steps and discarding the first 10 000 samples as burn-in. The reliability was evaluated by the effective sample size (ESS) and the mean TMRCA was obtained in TRACER.

We also estimated divergence time using the isolation-with-migration model implemented in IMa2 (Hey 2010), which allows for gene flow during lineage divergence. As with the BEAST analyses, only mtDNA loci were used because the mutation rates of microsatellites are highly uncertain and little evidence could be employed to estimate them in this species. The HKY model and 0.25 as inheritance scalar were used. Following the recommendations of Hey & Nielsen (2004), we first performed multiple short runs with an increasing number of steps and wide priors and heating schemes to ensure that the complete posterior distribution could be obtained. Final runs consisted of 1×10^8 steps with a burn-in of 1×10^7 steps. High ESS values (>1000) and similar parameter values estimated from two sets of runs demonstrated that the MCMC explored the parameter space sufficiently. Marginal histograms were also evaluated and compared to ensure consistent parameter estimates.

As no *Lophura* fossil data were available to calibrate the mutation rate, the rate of 1.19% per lineage per million years for cyt *b* (Weir & Schluter 2008) was used, as this is the only calibrated Galliform-specific mitochondrial gene

mutation rate available. The mutation rate of CR was calculated using GENALEX 6.2 (Peakall & Smouse 2006) by multiplying it with the ratio of the average genetic distance to cyt *b*.

Morphological clustering

We analysed a total of 99 adult male *L. nycthemera* specimens including all nine subspecies distributed in China (*fokiensis* = 7, *nycthemera* = 35, *rongjiangensis* = 11, *omeiensis* = 3, *whiteheadi* = 3, *beaulieui* = 10, *jonesi* = 9, *occidentalis* = 12, *rufipes* = 9; details available at Dryad doi: 10.5061/dryad.7kd74). In accordance with the morphological taxonomic criteria described by Delacour (1948) and Cheng (1978), five size measurements and four plumage pattern variables were used. Wing chord length (WL), tail length (TL) and pure white length of central rectrix (PWL) were measured with a long ruler to the nearest 1 mm. A caliper with a precision of 0.1 mm was used to measure bill length (BL) and tarsus length (TaL). We counted the number of black stripes on feathers of the hind neck (N_{hn}), mantle (N_m), rump (N_r) and lesser coverts (N_c). All measurements were taken by LD for consistency. The ratio of PWL/TL was calculated as the pure white tail length proportion (WP) to replace PWL in subsequent analyses.

Principal component analysis (PCA) was employed as a multivariate technique to visualize the morphological relationships among subspecies. We ran separate PCAs using different variable sets: the first used N_{hn}, N_m, N_r, N_c and WP to inspect the relationships of plumage patterns; the second used length characteristics, including WL, TL, BL and TaL, to examine body size clustering. All nine variables were pooled in a final PCA to examine the overall relationships.

Results

Genetic polymorphism

Sequencing of the two mtDNA segments with a joint alignment length of 2151 bp in 133 *L. nycthemera* individuals resulted in 79 haplotypes defined by 156 segregating sites (145 transitions and 22 transversions, with 22 singletons and 134 parsimony informative sites). For the 10 Kalij Pheasant samples collected in Yingjiang, eight haplotypes were identified based on 23 segregating sites (19 transitions and four transversions, with five singletons and 18 parsimony informative sites).

A total of 180 individuals (170 samples of Silver Pheasants and 10 Kalij Pheasants) were genotyped for 11 microsatellite loci (Table S1, Supporting information). Two individuals had more than three missing loci and were excluded. For the remaining data set, there were 19 missing genotypes (<1%) in different individuals. The mean number of alleles per population ranged from 3.73 (ZJ) to 9.36 (YJ) (Table 1). Expected heterozygosity varied from 0.49 (HN) to 0.73 (PW) and observed heterozygosity varied from 0.40 (HN) to 0.66 (PW). In general, the western populations and Sichuan populations (including HY and LJS belonging to *L. n. omeiensis*) showed greater diversity than the eastern populations and Hainan population (Table S1, Supporting information). The locus P5 deviated consistently from Hardy–Weinberg equilibrium with null alleles in all population samples and was thus excluded from further analyses. All the 10 remaining loci showed no significant deviation from linkage equilibrium.

Phylogeographic structure

At the population level, nine sampling localities had at least five individuals for which concatenated mtDNA sequences were available: WYS, GS, HU, LJS, HN, NE, BN, CY and YJ. Haplotype diversity was high in all populations (*Hd* = 0.752–1), but the mean nucleotide diversity (π) varied among populations (Table 1): the lowest π value was found in Hainan (0.122%) and the highest in Yingjiang (1.669%); eastern populations (WYS, GS, HU) showed lower diversity (0.168–0.171%) than western populations (NE, BN and CY, 0.262–0.366%). A very high global Φ_{ST} value of 0.83 ($P < 0.001$) was observed among the populations. Lower pairwise Φ_{ST} values were found between geographically closer populations (e.g. 0.054 for GS–WYS, 0.091 for BN–CY) and higher Φ_{ST} values between more distant comparisons (e.g. 0.897 for GS–BN and 0.890 for WYS–BN; Table S2, Supporting information).

The global F_{ST} value of 0.18 ($P < 0.001$) implies deep genetic divergence in the nuclear genome among the populations. Lower pairwise F_{ST} values between close populations (0.035–0.099 among populations, 0.005–0.084 among western populations) ranged up to 0.404 for populations farther apart (Table S2, Supporting information). The isolated Sichuan populations showed higher degrees of differentiation from eastern populations (from 0.085 to 0.125) than from western populations (0.033–0.085). The Hainan population had strikingly high F_{ST} values (0.272–0.404) about three times larger than most other comparisons.

The HKY+I+G model of nucleotide substitution with a proportion of invariant sites of 0.77 and a gamma shape parameter of 0.568 was selected for the concatenated sequence data using jModeltest. All phylogenetic analyses based on Bayesian, maximum-likelihood and maximum parsimony algorithms consistently yielded five haplogroups (Fig. 2). Four of these (the East, Sichuan, Hainan and West clades) corresponded to distinct geographic areas, but remarkably, one highly divergent

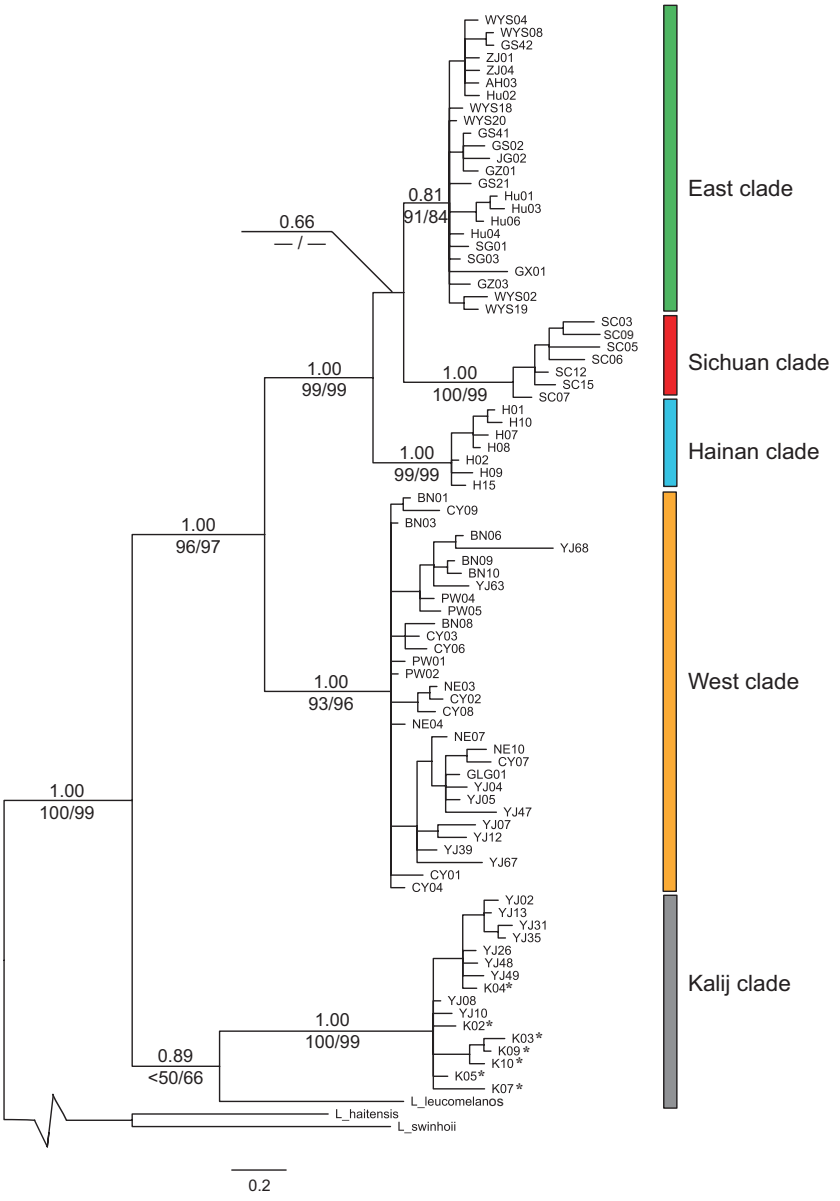

Fig. 2 Bayesian tree constructed from concatenated mitochondrial haplotypes (2051 bp, HKY+I+G model) showing phylogenetic relationships of Silver Pheasant (*Lophura nycthemera*) in China with three out-group species, *L. leucomelanos* (including seven haplotypes from Yingjiang labelled with '*' and one sequence from GenBank), *L. swinhoii* and *L. hatinhensis*. Numbers above branches indicate Bayesian posterior probabilities, and bootstrap values generated from ML (below branch, first) and MP (below branch, second) analyses are shown at the main nodes. Five major haplogroup classifications are given on the right.

clade composed of 12 sequences from Yingjiang [denoted as a distinct population, Yingjiang-Kalij (YJK)] was grouped as a sister clade to the Kalij Pheasant *L. leucomelanos* (the Kalij clade). No shared haplotypes were identified among the nine subspecies except one shared by *L. n. fokiensis* and *L. n. rongjiangensis* (haplotype WYS20 in Fig. 2), and each subspecies was contained within a distinct clade except *L. n. rufipes*. The East clade contained three subspecies (*L. n. fokiensis*, *L. n. nycthemera*, *L. n. rongjiangensis*) distributed between the Red and Yangtze rivers. The Sichuan clade was represented by subspecies *L. n. omeiensis*, distributed north of the Yangtze River and the Hainan clade contained only *L. n. whiteheadi* on Hainan Island. The West clade was composed of three additional subspecies (*L. n. beaulieui*, *L. n. jonesi*, *L. n. occidentalis*) and 18 of 30 sequences from Yingjiang (recognized as *L. n. rufipes*) distributed on the west side of the Red River. The other 12 samples of *L. n. rufipes* clustered with sympatric Kalij Pheasants. The median-joining network also grouped haplotypes into five clusters (Fig. S1, Supporting information), in agreement with the phylogenetic trees.

Haplotypes from the East, Sichuan and Hainan clades formed a monophyletic cluster with high support values. In the Bayesian topology, Sichuan and East sequences formed a monophyletic lineage (Fig. 2), but ML and MP analyses inferred that Sichuan and Hainan had closer relationships. Both alternative topologies were not well supported (lower than 0.7 in BPP, aLRT, and BP). The West clade was also supported by high

values, but no genetic structure was found within the lineage (Fig. 2).

PCoA based on microsatellite data revealed a clear separation of the genotypes of Hainan Island pheasants from the continental individuals by the first axis (Fig. 3). In total, 58.80% of the variation was explained by the first two ordination axes. The PCoA on the continental populations only indicated two clusters of East and West, with all Kalij Pheasants and most of the Sichuan individuals included in the West cluster (details not shown). The first two axes still explained 48.23% of the total variation.

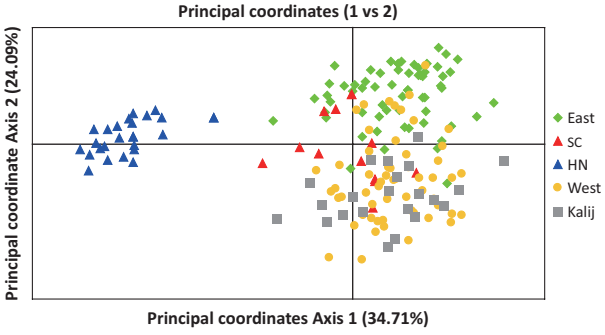

Fig. 3 Plot of the first two coordinates from principal coordinate analysis (PCoA) based on Euclidian distances from 10 microsatellite loci (n = 178). The first coordinate of the PCoA revealed two main clusters corresponding to Hainan Island and the continent and explained 34.71% of the variance. The second coordinate generally corresponded to east–west divergence and explained 24.09% of the variance. Different symbols represent different mtDNA lineages (see legend of Fig. 2 for details).

In our 10 independent Bayesian structure analyses to estimate K, the values of LnP(D) increased sharply from K 1 to 3, and ΔK had a prominent peak at K = 3 (Fig. S2, Supporting information). Under the optimal number of genetic clusters K = 3, continental populations separated into two distinct clusters: individuals from East populations (ZJ, WYS, GS and HU) formed a cluster together with some individuals from SC, and West populations (BN, NE and CY) formed another cluster along with most individuals from SC (Fig. 4). The assignment results for SC individuals were obviously different from mtDNA lineage affiliations (Fig. 4), which implied different evolutionary processes of mtDNA and nuclear loci. At K = 2, it was apparent that Hainan individuals formed the most distinct cluster, consistent with the results from PCoA. When we increased K to 4, the East and Hainan clusters maintained their integrity but west populations showed signs of admixture between Silver and Kalij Pheasants in Yingjiang. More than two-thirds of the Silver Pheasant individuals from Yingjiang were assigned to a different nuclear genetic background consistent with Kalij Pheasants. However, these were not exactly the same individuals contained in the Kalij clade according to mtDNA.

AMOVA analyses showed significant genetic variance among the five phylogeographic groups for both mtDNA (86.58%, $P < 0.01$) and microsatellite data (16.06%, $P < 0.01$). However, when the populations were grouped according to the island-continent situation, the explained proportion of variance rose for the microsatellite data (19.2%, $P = 0.056$) and dropped for mtDNA (-0.036; Table 2).

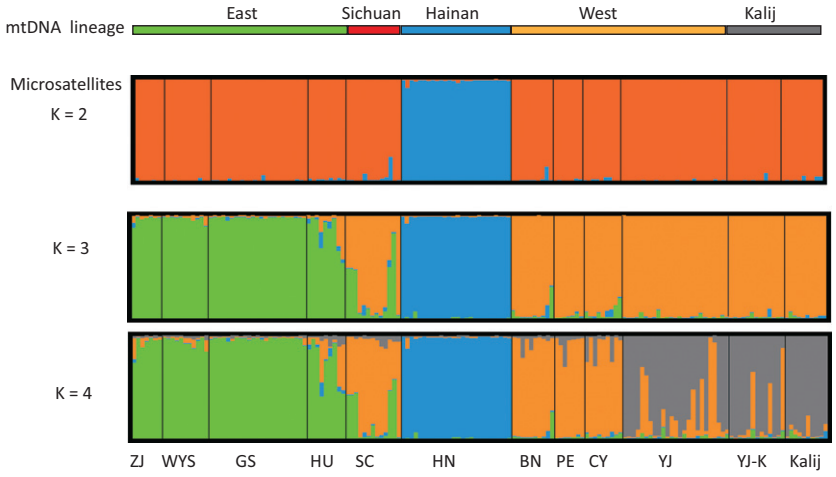

Fig. 4 Posterior assignment probabilities of Silver Pheasants from 10 populations (n = 153) combined with 10 Kalij Pheasants collected in Yingjiang. Different numbers of clusters (K = 2, 3, and 4) as determined by a Bayesian algorithm implemented in the program STRUCTURE v2.3.1. K = 3 was selected as the most likely number of clusters under the ln$K$ and ΔK comparison. The population name is shown below (corresponding to Table 1; YJ-K labels the Silver Pheasant samples in Yingjiang that clustered in the mtDNA Kalij clade) and mitochondrial lineages (East, green; Sichuan, red; Hainan, blue; West, orange; Kalij, black) are shown above each histogram.

Table 2 Analysis of molecular variance (AMOVA) results for mitochondrial DNA and microsatellite data. For each data type, five groups of populations were assigned according to evolutionary lineages of mtDNA sequence data (see Fig. 2), and two were assigned corresponding to island–continent isolation

Source of variation	Grouping	d.f.	% of total variation	Fixation indices
Mitochondrial DNA				
Among groups	mtDNA clade[†]	4	86.58	0.8658**
Among populations within groups		11	2.46	0.1833**
Within populations		120	10.96	0.8904**
Among groups	Island-Continent[‡]	1	−3.65	–0.0365
Among populations within groups		14	90.27	0.8709**
Within populations		120	13.38	0.8662**
Microsatellites				
Among groups	mtDNA clade	4	16.06	0.2079**
Among populations within groups		11	4.74	0.0564*
Within populations		330	79.20	0.1606**
Among groups	Island-Continent	1	19.20	0.1920
Among populations within groups		14	10.52	0.1301**
Within populations		330	70.29	0.2971**

*$P < 0.05$; **$P < 0.01$.
[†]mtDNA lineage: [AH,ZJ,WYS,GS,HU,JG,GZ][HN][SC][PE,PW,BN,YJ,CY][KP,YJK].
[‡]Island-Continent: [AH,ZJ,WYS,GS,HU,JG,GZ,SC,PE,PW,BN,YJ,CY,KP,YJK] [HN].

Demographic history and divergence time

Neutrality tests and mismatch analyses were conducted based on mtDNA lineages of Silver Pheasants (East, Hainan, Sichuan and West) (Table 3). Consistent results were found in the Sichuan clade (Tajima's $D = -0.075$, $P = 0.508$; Fu's $F_s = 1.303$, $P = 0.748$) compatible with mutation-drift equilibrium in the current population. In contrast, discordant results were found in the East, Hainan and West clades: Tajima's D values were not significant but Fu's F tests rejected mutation-drift equilibrium in these populations (East: Fu's $F = -10.08$, $P < 0.001$; Hainan: Fu's $F = -15.731$, $P < 0.001$; West: Fu's $F = -14.69$, $P < 0.001$). Mismatch distributions were unimodal in all clades (P-value of SSD, East, 0.625; Hainan, 0.725; Sichuan, 0.050; West, 0.401), consistent with historical demographic expansions in these populations. Approximate estimates for when the population expansion of the main mtDNA clades started according to τ yielded a range from 59 Kyr BP (Hainan clade) to 180 Kyr BP (Kalij clade) (Table 3).

Analyses of mtDNA sequences using BEAST indicated two main divergence events within the Silver Pheasant (Table 4): the West clade first diverged from the other clades about 0.66 Myr BP (95% CI, 0.432–0.901 Myr BP), and then, the three clades located east of the Red River diverged at a similar time around 0.3 Myr BP (Table 4). Remarkably, the divergence time between Silver (without YJK samples) and Kalij Pheasants was 1.087 Myr BP (95% CI: 0.7421–1.4799 myr BP), which is consistent with the TMRCA of Silver Pheasants including YJK samples, indicating again that it is unlikely that YJK haplotypes originated from the Silver Pheasant. The nonsignificant distribution of the standard deviation of the molecular clock (ucld.stedev = 0.273) suggested that there is a substantial clock-like rate among lineages. The estimated time of basal divergence (0.785 Myr BP; 95% CI, 0.505–0.959 Myr BP) and East–Sichuan divergence (0.369 Myr BP, 95% CI: 0.192–0.556 Myr BP) obtained from IMa2 was similar to BEAST estimates, but the island–continent divergence time estimated by IMa2 (0.558 Myr BP; 95% CI, 0.298–0.868 Myr BP) was somewhat older. Estimated population migration rates from IMa2 were not significantly different from zero.

Morphological clusters

Three PCAs based on data from 99 males were performed. The overall PCA on plumage and length variables revealed marked differences among the samples analysed (Fig. 5), largely consistent with the PCoA results of microsatellite data. The two main components explained 54% of the variation with the first component largely representing stripe numbers on the back and tail length, whereas the second component mainly represented the pure white ratio on the central rectrix and wing length. The three Hainan specimens were clearly separated from all continental specimens, and the continental samples were generally divided into two clusters, represented by subspecies distributed in the east (open symbols) and the west (black symbols). The PCA on plumage variables only (Fig. S3a, Supporting information; 74.9% of the variation explained) showed a similar patterns to the overall PCA, with PC1

Table 3 Summary statistics and results of demographic analyses for evolutionary lineages in Silver Pheasant mtDNA (CR+cyt *b*)

mtDNA lineage	Sample size	N_H	$H \pm$ SD	$\pi \pm$ SD (%)	Tajima's D	Fu's F_s	SSD	τ	Expansion time (years)
'East'	48	30	0.9361 ± 0.0197	0.182 ± 0.103	−1.234	−10.0813*	0.003	4.083 (1.629–6.442)	83 644 (33 371–131 971)
'Sichuan'	13	7	0.9103 ± 0.0485	0.3392 ± 0.1909	−0.075	1.303	0.029	8.499 (3.816–11.881)	174 111 (78 175–243 394)
'Hainan'	14	8	0.9231 ± 0.0438	0.1226 ± 0.0781	0.166	−15.731*	0.004	2.908 (0.842–4.876)	59 573 (17 249–99 889)
'West'	44	31	0.963 ± 0.0193	0.3877 ± 0.2033	−1.303	−14.688*	0.006	7.956 (4.939–11.676)	162 987 (101 180–239 194)
'Kalij'	22	16	0.9567 ± 0.0293	0.3581 ± 0.1936	−0.388	−4.332	0.016	8.806 (4.845–12.511)	180 399 (99 254–256 300)

*$P < 0.05$.
NH, number of haplotypes; *H*, haplotype diversity; π, nucleotide diversity. SSD: sum-of-squared deviations estimated in mismatch analyses, τ: mode of mismatch distribution.

Table 4 The time to most recent common ancestor (TMRCA) estimated by BEAST and divergence time between different lineages in Silver Pheasant according to the isolation-with-migration model implemented in IMa2. 95% HPD represents the highest posterior density interval and is the most compact interval of the parameter that contains 95% of the posterior probability estimated

		Divergence time (Myr)		
Lineage divergence	Method	Mean	95% HPD lower	95% HPD upper
East/Sichuan	BEAST	0.311	0.202	0.441
	IMa2	0.369	0.192	0.556
East+Sichuan/Hainan	BEAST	0.317	0.192	0.440
	IMa2	0.558	0.298	0.868
East+Sichuan+Hainan/West	BEAST	0.655	0.432	0.901
	IMa2	0.785	0.505	0.959

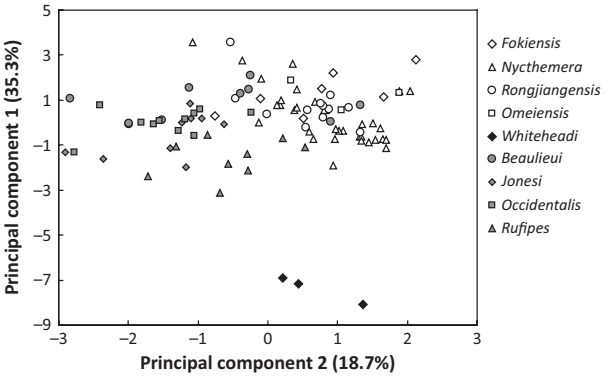

Fig. 5 Plot of first two coordinates from principal component analysis (PCA) of variation in nine morphological traits in 99 specimens of nine subspecies across China. Different symbols represent subspecies (see legend of Fig. 1 for details).

representing the number of stripes on the back and PC2 mainly representing the pure white ratio on the central rectrix. However, the PCA of size measurements did not show the same level of resolution (Fig. S3b, Supporting information) although *L. n. whiteheadi* and *L. n. rufipes* specimens showed somewhat higher scores in PC1.

Discussion

Phylogeographic structure and introgression

Phylogenetic reconstruction using mtDNA sequences identified a hierarchical genetic structure in Chinese Silver Pheasant, with a basal split dividing eastern (East, Hainan and Sichuan) and western (West) clades (Fig. 2), and signals in both mtDNA and nucDNA for polyphyletic arrangements in *L. n. rufipes* from the contact zone of Silver and Kalij Pheasants. The deep maternal genetic

structure of four clades recovered with tree-based methods matches the topological pattern in China, corresponding to the Southeast Hills, Sichuan Basin, Hainan Island and Yunnan Plateau, respectively (Fig. 1). This phylogeographic structure was also supported by the haplotype network (Fig. S1, Supporting information), AMOVA (Table 2) and Φ_{ST} values (Table S2, Supporting information). Contrary to the basal split, the order of divergence among the East, Sichuan and Hainan clades was not unambiguously resolved with all phylogenetic methods (Fig. 2), and mtDNA divergence may have occurred at similar times (Table 4). Individual-centred and population-based analyses of nuclear DNA revealed three highly supported genetic clusters, which generally corresponded to the maternal phylogenetic clades East, Hainan and West, while admixture between eastern and western populations and cytonuclear discordance (Figs 3 and 4) was observed in some Sichuan individuals which appeared undifferentiated morphologically (Fig. 5). Recent studies show that genetic introgression of mtDNA and cytonuclear discordance of allopatric or parapatric lineages is a relatively common phenomenon in various taxa (e.g. Petit & Excoffier 2009; Bastos-Silveira *et al.* 2012; Kindler *et al.* 2012; Sutter *et al.* 2013).

Cytonuclear discordance in the two isolated phylogeographic clades, Sichuan and Hainan, was demonstrated by the comparison of the geographic patterns in mtDNA, nucDNA and morphotypes. Comparatively deeper divergence between Hainan Island pheasants and continental populations was estimated based on nuclear loci compared to mtDNA with very high pairwise F_{ST} (Table S2, Supporting information) and isolated clustering in PCoA and Structure analyses (Figs 3 and 4). Considering the distinct morphological characters (Fig. 5), local adaptation might play an important role in the unique pattern but genetic drift cannot be excluded. In contrast, Sichuan populations north of the Yangtze River formed a monophyletic lineage in mtDNA, but showed higher genetic diversity and evidence of admixture in the nuclear genome. Although near-zero maternal gene flow was estimated using IMa2, male-mediated gene flow with other subspecies might explain the discrepancy between mtDNA and nuclear loci in the Sichuan pheasants (see e.g. Braaker & Heckel 2009; Kindler *et al.* 2012). A cline in the ratio of black on the outer tail feathers (Dong & Zhang 2011) in the subspecies *L. n. whiteheadi* (Hainan clade), *L. n. rongjiangensis*, partially *L. n. nycthemera* pheasants (East clade), and the Sichuan clade may indicate a common ancestor or male-mediated historical gene flow between these populations. As microsatellites have a larger effective population size than mtDNA sequences (Ellegren 2004; Zink & Barraclough 2008), the alternative scenario—that the signs of admixture were induced by incomplete sorting of nuclear loci—cannot be rejected completely. There have been few previous studies regarding the phylogenetic patterns of birds across the Yangtze River, but for example in *Alcippe morrisonia* (Song *et al.* 2009) and *Leucodioptron canorum* (Li *et al.* 2009), there is no deep mtDNA divergence as in the Silver Pheasant.

With regard to individuals from Yingjiang, our results demonstrate that the population of the subspecies *L. n. rufipes* as defined by previous taxonomy (Delacour 1948; Cheng 1978) clearly contains a mixture of two divergent lineages for both mitochondrial and nuclear DNA (Figs 2 and 4). The *L. n. rufipes* birds closely resemble Silver Pheasants in male plumage traits (including black and white stripes on the upper plumage, and red tarsus and feet), but also have some unstable Kalij-like morphological characters, such as a dark blue rump and black tail. Together this strongly suggests that this population and potentially the entire subspecies *L. n. rufipes* represents a hybrid population of Silver and Kalij Pheasants and not a distinct evolutionary lineage. Kalij Pheasants have been reported to be distributed to the west of the Irrawaddy River (Delacour 1948; del Hoyo *et al.* 1994) allopatric with Silver Pheasants on the east side of the river. However, the sympatric occurrence of these two pheasants is supported by specimen evidence (Cheng 1978) and our field observations. Demographic analyses did not provide evidence of a historical expansion of the Kalij mtDNA clade (Table 3), but the secondary contact between the sister species in Yingjiang could also be the result of a recent eastward expansion of Kalij Pheasants. Since the late Pliocene, the genus *Lophura* has rapidly diverged into 10 species (Randi *et al.* 2001) for which reproductive isolation is not always complete. For example, *L. imperialis* resulted probably from hybridization between Silver and Edward's Pheasants (*L. edwardsi*)(Hennache *et al.* 2003). The presence of potential hybrids with Silver and Kalij Pheasant mtDNA (Fig. 4) and the differences in male plumage between the parental taxa suggest that it would be interesting to investigate the mechanisms of mate recognition and mate choice and the consequences of natural hybridization further. The occurrence and consequences of hybridization have been widely studied in North American and European birds (e.g. Dyke *et al.* 2003; Peters *et al.* 2007; Brelsford *et al.* 2011; Hermansen *et al.* 2011), but except for the probably human-induced introgression of Hwamei (*Leucodioptron canorus*) in Taiwan (Li *et al.* 2010), little is known from the Chinese region.

The unsampled further subspecies of the Silver Pheasant in Southeast Asia prevent us from drawing wider conclusions about the phylogeography and lineage admixture at the species level. However, a previous phylogenetic reconstruction based on mtDNA covering five subspecies, which included three from Southeast

Asia suggested a basal divergence between the south-west (*L. n. jonesi*, *L. n. lewisi*, *L. n. annanmensis*) and north-east (*L. n. nycthemera* and *L. n. berliozi*) taxa (Moulin *et al.* 2003). This is consistent with the divergence patterns in our samples from China, but dedicated sampling of more Southeast Asian populations will be necessary to explore phylogeographic and hybridization patterns in the tropical regions. Coverage of the southern part of the contact zone between the Silver and Kalij Pheasants in west Thailand would be particularly interesting to determine the geographic spread of current and historical hybridization between these taxa.

Biogeography and divergence time

Our estimates suggest a basal divergence of Silver Pheasants in China approximately 0.66–0.78 Myr BP. This coincides with the marine isotope stages (MIS) 16–18 (0.6–0.7 Myr BP) or Kunlun glaciation in China, which had the largest glacial extension in the Pleistocene according to δ^{18} O values and pollen data (Zhao *et al.* 2011). No further phylogeographic pattern was revealed in the West populations, but the high degree of genetic diversity (Table 1) and evidence of an expansion around 0.16 Myr BP (Table 3) may indicate that there was a relatively large refugial area or many smaller interconnected ones at least during the last glaciation. The substantial divergence of eastern populations was estimated about 0.3–0.5 Myr BP, corresponding to MIS 8 or the first phase of the penultimate glaciation in China (0.3–0.4 Myr BP; Yi *et al.* 2005). The estimated expansion time of the East clade corresponds to the last long interglacial period in China (MIS 5, 75–125 Kyr BP; Zhang *et al.* 2006), which also points to relatively mild effects of the last glaciation on these populations. Southern China was not covered by continental ice sheets during the Pleistocene, but it experienced repeatedly substantial vegetation changes (Harrison *et al.* 2001). However, the topographic complexity of the region has apparently provided enough refugial habitats for the survival of the different clades during the last glaciation, and morphological diversification within clades is compatible with the partial restriction of gene flow between different regions and refugia with different ecological conditions.

The basal divergence between the East, West and the Sichuan lineages occurred apparently much later than the formation of some potential river barriers. The Red River represents the boundary between continental China's subtropical and tropical forests (Li & Li 1997) and also between the current distributions of the East and West lineages. The Red River once experienced intensive geological activities due to the uplift of the Himalayan Mountains, but its middle and lower watercourses were relatively stable already in the middle Pleistocene (~1.5 Myr BP). This time is considerably earlier than the TMRCA and the estimated divergence time between western and eastern populations (0.66 and 0.79 Myr BP; Table 4). With regard to a barrier between the Sichuan and East clades, the Yangtze River was similarly affected by the geological and climatic changes in the Pleistocene and it had also obtained its current position well before the estimated divergence time 0.31 Myr BP between the Sichuan and East clades. It is thus unlikely that barrier effects of these rivers caused the separation of the lineages but rather that it is a consequence of separate refugial areas associated with the repeated climatic changes in the region. Nevertheless, these major rivers may reduce gene flow to some extent even though pheasants are relatively mobile birds. Dedicated investigations would be necessary to quantify the extent of dispersal events across rivers specifically, but there are three nominal subspecies (*L. n. jonesi*, *L. n. beaulieui*, *L. n. occidentalis*) within the western range of our investigations that are separated by major rivers such as the Lancang-Mekong and Nujiang-Salween (Delacour 1948; Cheng 1978). No particular genetic structures or morphological clusters were detected among these populations, which is compatible with a relatively weak restriction of historical gene flow across these rivers.

Estimated divergence of the Hainan clade from the analysed continental clades (Table 4) clearly predates the beginning of the current physical separation of the insular population from its continental relatives by the Qiongzhou Strait after the last glaciation. Hainan Island was repeatedly connected and disconnected from the continent during the Pleistocene (Voris 2001), which has probably allowed its original colonization by pheasants. Although a large land surface emerged between Hainan Island and the mainland with the retreat of the sea during the glaciations, the flora in this area is thought to have been temperate deciduous broad-leaved forest and steppe rather than evergreen broad-leaved forest during the last glaciation (Voris 2001). The absence of appropriate habitats for the species in this region may have strongly restricted gene flow between the Hainan and mainland populations despite physical connection and thus allowed the evolution of genetic and morphological distinctness of *L. n. whiteheadi*.

It is important to keep in mind, however, that the origin of the Silver Pheasants colonizing Hainan is not entirely clear. The current population is about equally distinct from the West and East clades for nuclear DNA and somewhat closer to the East clade for mtDNA, but lower sea levels might have also provided the possibility for the colonization of Hainan from the west rather than the north. A critical test of these two possibilities cannot

be undertaken without examination of the yet unsampled subspecies on the Indo-Chinese peninsula. Such an extension of the analyses would certainly further our understanding of the phylogeographic processes in the Silver Pheasant, and it would also contribute to a better characterization of the evolutionary history of this biodiversity hotspot region.

Acknowledgements

We acknowledge the following people for their help in obtaining samples for this study: Limin Feng, Li Li, Aiwu Jiang and Yue Sun. We are grateful to the following institutions and people for help in specimen examination and literature: Museum of Institute of Zoology, Chinese Academy of Sciences (CAS), Beijing; Museum of Kunming Institute of Zoology, CAS, Kunming; Natural History Museum, London; Museum national d'Histoire Naturelle, Paris; P. McGowan and M. Adams. We thank Zhenting Zhou, Yang Liu, Susanne Tellenbach and Eveline Kindler for technical assistance, and the Berne University Research foundation for support. This project was supported by the National Natural Science Foundation of China (No. 30970377 and No. 31101627), the Fundamental Research Funds for the Central Universities to LD and YYZ and Program for New Century Excellent Talents in University (NCET-10-0111) to WL.

References

Aleixo A (2004) Historical diversification of a terra-firme forest bird superspecies: a phylogeographic perspective on the role of different hypotheses of Amazonian diversification. *Evolution*, **58**, 1303–1317.

Anisimova M, Gascuel O (2006) Approximate likelihood-ratio test for branches: a fast, accurate, and powerful alternative. *Systematic Biology*, **55**, 539–552.

Anthony N, Johnson-Bawe M, Jeffery K *et al.* (2007) The role of Pleistocene refugia and rivers in shaping gorilla genetic diversity in central Africa. *Proceedings of the National Academy of Sciences of the USA*, **104**, 20432–20436.

Bandelt H-J, Forster P, Rohl A (1999) Median-joining networks for inferring intraspecific phylogenies. *Molecular Biology and Evolution*, **16**, 37–48.

Bastos-Silveira C, Santos SM, Monarca R, Mathias MDL, Heckel G (2012) Deep mitochondrial introgression and hybridization among ecologically divergent vole species. *Molecular Ecology*, **21**, 5309–5323.

Bowen G, Clyde W, Koch P *et al.* (2002) Mammalian dispersal at the Paleocene/Eocene boundary. *Science*, **295**, 2062.

Braaker S, Heckel G (2009) Transalpine colonisation and partial phylogeographic erosion by dispersal in the common vole *Microtus arvalis*. *Molecular Ecology*, **18**, 2518–2531.

Brelsford A, Mila B, Irwin DE (2011) Hybrid origin of Audubon's warbler. *Molecular Ecology*, **20**, 2380–2389.

Cheng TS (1978) *Fauna Sinica, Series Vertebrata, Aves, Vol. 4: Galliformes*. Science Press, Beijing.

Cheng J, Liu X, Gao Z, Tang D, Yue J (2001) Effect of the Tibetan Plateau uplifting on geological environment of the Yunnan Plateau. *Geoscience*, **15**, 290–296.

Crowe T, Bowie R, Bloomer P *et al.* (2006) Phylogenetics, biogeography and classification of, and character evolution, in gamebirds (Aves: Galliformes): effects of character exclusion, data partitioning and missing data. *Cladistics*, **22**, 495–532.

Dai C, Zhao N, Wang W *et al.* (2011) Profound climatic effects on two East Asian black-throated tits (Aves: Aegithalidae), revealed by ecological niche models and phylogeographic analysis. *PLoS ONE*, **6**, e29329.

Delacour J (1948) The subspecies of *Lophura nycthemera*. *American Museum Novitates*, **1377**, 1–12.

Ding L, Gan X, He S, Zhao E (2011) A phylogeographic, demographic and historical analysis of the short-tailed pit viper (*Gloydius brevicaudus*): evidence for early divergence and late expansion during the Pleistocene. *Molecular Ecology*, **20**, 1905–1922.

Dong L, Zhang Y (2011) Intraspecific taxonomy study of Silver pheasant *Lophura nycthemera*. *Acta Zootaxonomica Sinica*, **36**, 431–446.

Drummond A, Rambaut A (2007) BEAST: Bayesian evolutionary analysis by sampling trees. *BMC Evolutionary Biology*, **7**, 214.

Dyke GJ, van Tuinen M (2004) The evolutionary radiation of modern birds (Neornithes): reconciling molecules, morphology and the fossil record. *Zoological Journal of the Linnean Society*, **141**, 153–177.

Dyke GJ, Gulas BE, Crowe TM (2003) Suprageneric relationships of galliform birds (Aves, Galliformes): a cladistic analysis of morphological characters. *Zoological Journal of the Linnean Society*, **137**, 227–244.

Ellegren H (2004) Microsatellites: simple sequences with complex evolution. *Nature Reviews Genetics*, **5**, 435–445.

Evanno G, Regnaut S, Goudet J (2005) Detecting the number of clusters of individuals using the software STRUCTURE: a simulation study. *Molecular Ecology*, **14**, 2611–2620.

Excoffier L, Laval G, Schneider S (2005) Arlequin (version 3.0): an integrated software package for population genetics data analysis. *Evolutionary Bioinformatics Online*, **1**, 47.

Fuchs J, Ericson P, Pasquet E (2007) Mitochondrial phylogeographic structure of the white-browed piculet (*Sasia ochracea*): cryptic genetic differentiation and endemism in Indochina. *Journal of Biogeography*, **35**, 565–575.

Guindon S, Gascuel O (2003) A simple, fast, and accurate algorithm to estimate large phylogenies by maximum likelihood. *Systematic Biology*, **52**, 696–704.

Hahne J, Jenkins T, Halle S, Heckel G (2011) Establishment success and resulting fitness consequences for vole dispersers. *Oikos*, **120**, 95–105.

Harrison S, Yu G, Takahara H, Prentice I (2001) Diversity of temperate plants in east Asia. *Nature*, **413**, 129–130.

Hayes F, Sewlal J (2004) The Amazon River as a dispersal barrier to passerine birds: effects of river width, habitat and taxonomy. *Journal of Biogeography*, **31**, 1809–1818.

Hennache A, Rasmussen P, Lucchini V *et al.* (2003) Hybrid origin of the imperial pheasant *Lophura imperialis* (Delacour and Jabouille, 1924) demonstrated by morphology, hybrid experiments, and DNA analyses. *Biological Journal of the Linnean Society*, **80**, 573–600.

Hermansen J, Saether SA, Elgvin N *et al.* (2011) Hybrid speciation in sparrows I: phenotypic intermediacy, genetic admixture and barriers to gene flow. *Molecular Ecology*, **20**, 3812–3822.

Hewitt G (2000) The genetic legacy of the Quaternary ice ages. *Nature*, **405**, 907–913.

Hewitt G (2004) Genetic consequences of climatic oscillations in the Quaternary. *Philosophical Transactions of the Royal Society of London. Series B: Biological Sciences*, **359**, 183.

Hey J (2010) Isolation with migration models for more than two populations. *Molecular Biology and Evolution*, **27**, 905–920.

Hey J, Nielsen R (2004) Multilocus methods for estimating population sizes, migration rates and divergence time, with applications to the divergence of *Drosophila pseudoobscura* and *D. persimilis*. *Genetics*, **167**, 747–760.

Howard W (1997) A warm future in the past. *Nature*, **388**, 418–419.

del Hoyo J, Elliott A, Sargatal J (1994) *Handbook of the Birds of the World, Vol. 2: New World Vultures to Guineafowl*. Lynx Edicions, Barcelona.

Huang Z, Liu N, Liang W *et al.* (2010) Phylogeography of Chinese bamboo partridge, *Bambusicola thoracica thoracica* (Aves: Galliformes) in south China: Inference from mitochondrial DNA control-region sequences. *Molecular Phylogenetics and Evolution*, **56**, 273–280.

Huelsenbeck J, Ronquist F (2001) MrBayes: a program for the Bayesian inference of phylogeny. *Bioinformatics*, **17**, 754–755.

Johnsgard P (1999) *Pheasants of the World*, 2nd edn. Oxford University Press, Oxford.

Kimball R, Braun E (2008) A multigene phylogeny of Galliformes supports a single origin of erectile ability in non-feathered facial traits. *Journal of Avian Biology*, **39**, 438–445.

Kindler E, Arlettaz R, Heckel G (2012) Deep phylogeographic divergence and cytonuclear discordance in the grasshopper *Oedaleus decorus*. *Molecular Phylogenetics and Evolution*, **65**, 695–704.

Ksepka D (2009) Broken gears in the avian molecular clock: new phylogenetic analyses support stem galliform status for *Gallinuloides wyomingensis* and rallid affinities for *Amitabha urbsinterdictensis*. *Cladistics*, **25**, 173–197.

Li X, Li J (1997) The Tanaka-Kaiyong Line – an important floristic line for the study of the flora of East Asia. *Annals of the Missouri Botanical Garden*, **84**, 888–892.

Li S, Yeung C, Feinstein J *et al.* (2009) Sailing through the Late Pleistocene: unusual historical demography of an East Asian endemic, the Chinese Hwamei (*Leucodioptron canorum canorum*), during the last glacial period. *Molecular Ecology*, **18**, 622–633.

Li J, Yeung C, Tsai P *et al.* (2010) Rejecting strictly allopatric speciation on a continental island: prolonged postdivergence gene flow between Taiwan (*Leucodioptron taewanus*, Passeriformes Timaliidae) and Chinese (*L. canorum canorum*) hwameis. *Molecular Ecology*, **19**, 494–507.

McGowan P, Panchen A (1994) Plumage variation and geographical distribution in the Kalij and Silver Pheasants. *Bulletin of the British Ornithologists' Club*, **114**, 113–123.

Moulin S, Randi E, Tabarroni C, Hennache A (2003) Mitochondrial DNA diversification among the subspecies of the Silver and Kalij Pheasants, *Lophura nycthemera* and *L. leucomelanos*, Phasianidae. *Ibis*, **145**, E1–E11.

Nicolas V, Missoup A, Denys C *et al.* (2011) The roles of rivers and Pleistocene refugia in shaping genetic diversity in *Praomys misonnei* in tropical Africa. *Journal of Biogeography*, **38**, 191–207.

Peakall R, Smouse P (2006) GenAlEx V6. 1: Genetic Analysis in Excel. Population genetic software for teaching and research. *Molecular Ecology Notes*, **6**, 288–295.

Peters JL, Zhuravlev Y, Fefelov I *et al.* (2007) Nuclear loci and coalescent methods support ancient hybridization as cause of mitochondrial paraphyly between gadwall and falcated duck (*Anas* spp.). *Evolution*, **61**, 1992–2006.

Petit RJ, Excoffier L (2009) Gene flow and species delimitation. *Trends in Ecology & Evolution*, **24**, 386–393.

Posada D (2008) jModelTest: phylogenetic model averaging. *Molecular Biology and Evolution*, **25**, 1253.

Pritchard J, Stephens M, Donnelly P (2000) Inference of population structure using multilocus genotype data. *Genetics*, **155**, 945.

Qvarnström A, Rice A, Ellegren H (2010) Speciation in *Ficedula* flycatchers. *Philosophical Transactions of the Royal Society B: Biological Sciences*, **365**, 1841–1852.

Rambaut A, Drummond A (2007) Tracer v1. 4. Available from http://beast.bio.ed.ac.uk/Tracer.

Randi E, Lucchini V (1998) Organization and evolution of the mitochondrial DNA control region in the avian genus *Alectoris*. *Journal of Molecular Evolution*, **47**, 449–462.

Randi E, Lucchini V, Hennache A *et al.* (2001) Evolution of the mitochondrial DNA control region and cytochrome *b* genes and the inference of phylogenetic relationships in the avian genus *Lophura* (Galliformes). *Molecular Phylogenetics and Evolution*, **19**, 187–201.

Rheindt F, Edwards S (2011) Genetic introgression: an integral but neglected component of speciation in birds. *The Auk*, **128**, 620–632.

Ronquist F, Huelsenbeck J (2003) MrBayes 3: Bayesian phylogenetic inference under mixed models. *Bioinformatics*, **19**, 1572.

Shen Y, Liang L, Sun Y *et al.* (2010) A mitogenomic perspective on the ancient, rapid radiation in the Galliformes with an emphasis on the phasianidae. *BMC Evolutionary Biology*, **10**, 132.

Song G, Qu Y, Yin Z *et al.* (2009) Phylogeography of the *Alcippe morrisonia* (Aves: Timaliidae): long population history beyond late Pleistocene glaciations. *BMC Evolutionary Biology*, **9**, 143.

Sutter A, Beysard M, Heckel G (2013) Sex-specific clines support incipient speciation in a common European mammal. *Heredity*, **110**, 398–404.

Swofford D (2001) *PAUP* 4.0 Beta 5: Phylogenetic Analysis Using Parsimony (and Other Methods)*. Sinauer Associates, Sunderland, Massachusetts.

Tamura K, Nei M (1993) Estimation of the number of nucleotide substitutions in the control region of mitochondrial DNA in humans and chimpanzees. *Molecular Biology and Evolution*, **10**, 512–526.

Tamura K, Peterson D, Peterson N *et al.* (2011) MEGA5: Molecular Evolutionary Genetics Analysis Using Maximum Likelihood, Evolutionary Distance, and Maximum Parsimony Methods. *Molecular Biology and Evolution*, **28**, 2731–2739.

van Tuinen M, Dyke G (2004) Calibration of galliform molecular clocks using multiple fossils and genetic partitions. *Molecular Phylogenetics and Evolution*, **30**, 74–86.

Vallender R, Robertson R, Friesen V, Lovette I (2007) Complex hybridization dynamics between golden winged and blue winged warblers (*Vermivora chrysoptera* and *Vermivora pinus*) revealed by AFLP, microsatellite, intron and mtDNA markers. *Molecular Ecology*, **16**, 2017–2029.

Voris H (2001) Maps of Pleistocene sea levels in Southeast Asia: shorelines, river systems and time durations. *Journal of Biogeography*, **27**, 1153–1167.

Weir J, Schluter D (2008) Calibrating the avian molecular clock. *Molecular Ecology*, **17**, 2321–2328.
Yi C, Cui Z, Xiong H (2005) Numerical periods of Quaternary glaciations in China. *Quaternary Sciences*, **25**, 609–619.
Zhang W, Cui Z, Li Y (2006) Review of the timing and extent of glaciers during the last glacial cycle in the bordering mountains of Tibet and in East Asia. *Quaternary International*, **154**, 32–43.
Zhang D, Chen M, Murphy R *et al.* (2010a) Genealogy and palaeodrainage basins in Yunnan Province: phylogeography of the Yunnan spiny frog, *Nanorana yunnanensis* (Dicroglossidae). *Molecular Ecology*, **19**, 3406–3420.
Zhang M, Rao D, Yang J *et al.* (2010b) Molecular phylogeography and population structure of a mid-elevation montane frog *Leptobrachium ailaonicum* in a fragmented habitat of southwest China. *Molecular Phylogenetics and Evolution*, **54**, 47–58.
Zhao J, Shi Y, Wang J (2011) Comparison between Quaternary glaciations in China and the Marine Oxygen Isotope Stage (MIS): an improved schema. *Acta Geographica Sinica*, **66**, 867–884.
Zhou Z, Zhang Y (2009) Isolation and characterization of microsatellite markers for Temminck's Tragopan (*Tragopan temminckii*). *Conservation Genetics*, **10**, 1633–1635.
Zink R, Barraclough G (2008) Mitochondrial DNA under siege in avian phylogeography. *Molecular Ecology*, **17**, 2107–2121.

Y.Z. and L.D. designed the overall scope of research. L.D., W.L. and Y.Z. carried out the field survey and collected pheasant samples across China. L.D. and G.H performed the laboratory work and molecular data analysis. L.D. measured specimen and conducted statistical analyses under guidance of G.H. and W.L.. All authors contributed to the writing of the manuscript.

Data accessibility

GenBank accession numbers of DNA sequences, morphological data and microsatellite genotypes: Dryad doi: 10.5061/dryad.7kd74.

Supporting information

Additional supporting information may be found in the online version of this article.

Fig. S1 Unrooted median-joining networks of the concatenated mtDNA sequence of Silver Pheasants (n = 133) and Kalij Pheasants (n = 10).

Fig. S2 Results from 10 independent replicate runs each of the software STRUCTURE for the estimation of K.

Fig. S3 Plots of first two axes from principal components analyses (PCA) based on (a) four size measurement variables and (b) five plumage pattern variables in 99 specimens of nine subspecies of Silver Pheasant across China.

Table S1 Genetic variability at 11 microsatellite loci per population and overall.

Table S2 Pairwise genetic differentiation among populations: Φ_{ST} (mtDNA, below diagonal) and F_{ST} (STR, above diagonal).

Data files: DNA alignments of mtDNA sequences (control region and cyt *b*) and input file of IMa2.